N.I.

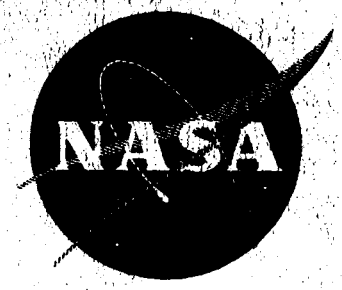

PROGRESS REPORT NO. 6

14 February 1968 to 14 May 1968

TOTAL ENERGY DISTRIBUTION MEASUREMENTS OF FIELD EMITTED ELECTRONS

BY

L. W. Swanson
L. C. Crouser

Prepared for

Headquarters

National Aeronautics and Space Administration
Washington, D. C.

June 1968

Contract NASw-1516

Field Emission Corporation

McMinnville, Oregon

PROGRESS REPORT NO. 6

14 February 1968 to 14 May 1968

TOTAL ENERGY DISTRIBUTION MEASUREMENTS OF FIELD EMITTED ELECTRONS

By

L. W. Swanson
L. C. Crouser

Prepared for

Headquarters
National Aeronautics and Space Administration
Washington, D. C.

June 1968

CONTRACT NASw-1516

TABLE OF CONTENTS

ILLUSTRATIONS

ILLUSTRATIONS (Cont'd)

TABLES

PURPOSE

The purpose of this research program is two-fold. First, we are interested in measuring the total energy distribution of field emitted electrons in order to ascertain the usefulness of this technique to examine the electronic band structure. During this program we plan to extend the measurements to various orientations of different metals. The second thrust of this program involves an investigation of the effect of adsorption on the total energy distribution. According to recent theoretical studies one may expect to obtain information regarding the nature of the bonding mechanism from such studies.

I INTRODUCTION

A new concentric sphere retarding potential energy analyzer tube has been constructed and is awaiting evacuation. It is planned to first check operation and resolution of the tube with a <310> oriented W field emitter since the electron emission behavior of that direction is well known and predictable. It is then hoped to extend these measurements to other metals in which solid state band structure measurements have indicated a possibility of field emission total energy distribution (TED) measurements elucidating the band structure information.

A preliminary study of the effect of adsorbed layers on TED measurements and total current-voltage relationships has been completed. The TED of field emitted electrons from single crystal faces of cesium and barium coated tungsten and molybdenum surfaces have been measured. The various experimental parameters extracted from TED curves were compared with theoretical values obtained from the Sommerfeld based Fowler-Nordheim theory of field emission by assuming the adsorbate alters the emission through the work function term. Results of adsorption on (111) Mo, (110) Mo, and (110) W are in reasonable agreement with the Fowler-Nordheim theory so far as the TED shapes are concerned. A decrease of the apparent emitting area with adsorbate coverage can be explained by a field polarization effect. However, a sharp increase in the apparent emitting area at low cesium coverages may be due to a resonance tunnelling effect as predicted elsewhere.

II THE MODIFIED CONCENTRIC SPHERE RETARDING POTENTIAL ANALYZER

During this period a great deal of effort has gone into the design and construction of a concentric sphere retarding potential analyzer. A schematic diagram of the new lens system is shown in Figure 1. Several modifications have been made in the present design when compared to the analyzer reported on during the last period. An electrode A (Figure 1) has been added to the system in order to couple the accelerating lens closer to the cathode. By

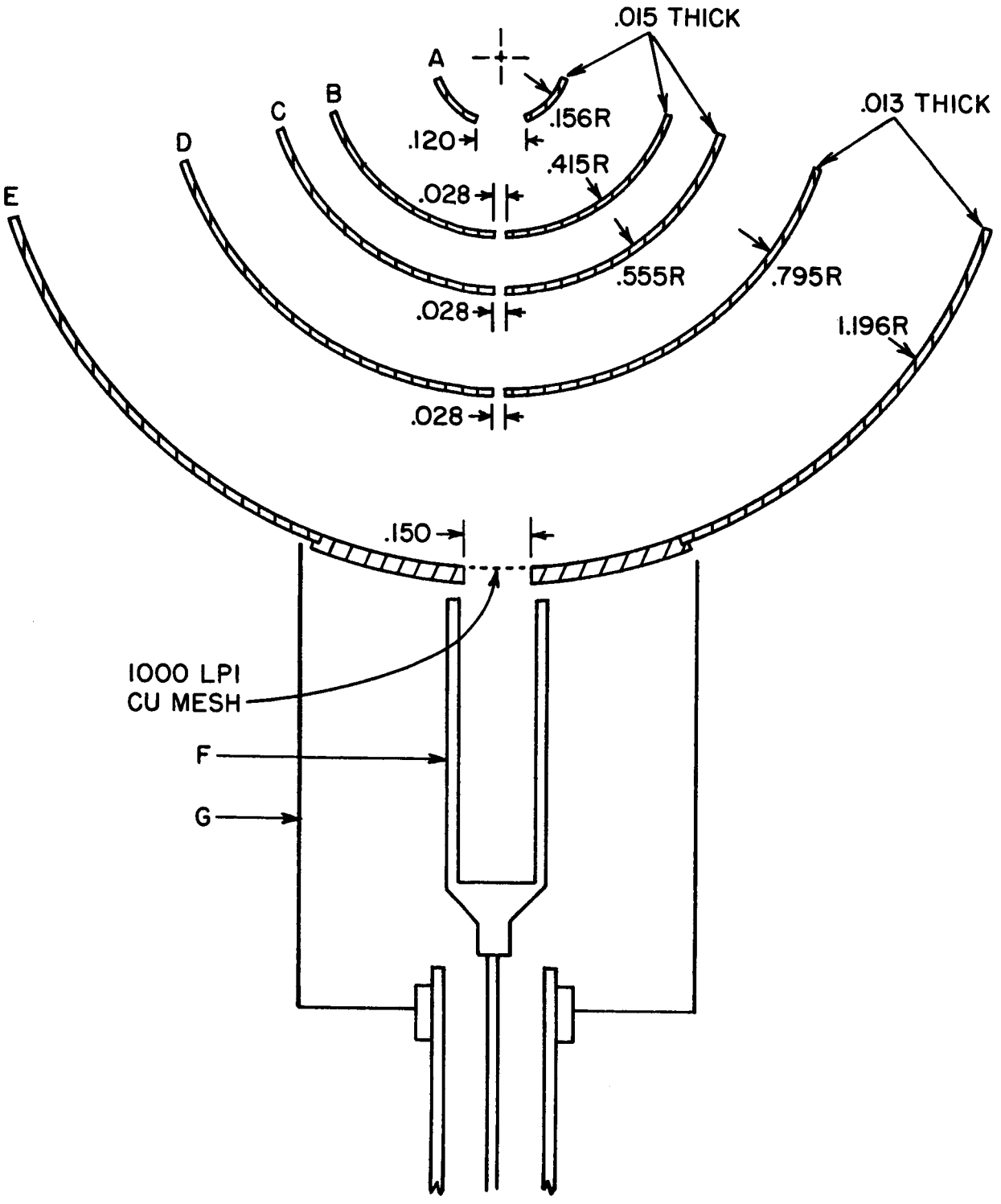

Figure 1. Lens system in modified concentric sphere retarding potential energy distribution tube consisting of lens system (A - E), collector (F) and ground shield (G).

doing this it will be possible to operate the system at a lower total voltage because of the closer spacing. We also have attempted to reduce any lens effects occurring at electrodes B, C, and D by reducing the aperature sizes. The single crystal collector in the previous design has been replaced by a mesh and Faraday cup so that only those electrons passing through the mesh and into the Faraday cup are analyzed. It is expected that this method of collection will overcome the problem of the reflection of low energy electrons from the collector surface. The Faraday cup can be biased slightly positive with respect to the mesh so any reflected electrons from the Faraday cup will be forced to return to the cup and be collected.

The necessary considerations in the design of a concentric sphere retarding analyzer were pointed out in the last report and involved determining the proper voltage for the spherical electrodes of radius r according to

$$V(r) = \frac{R}{R-r_o}\left(1 - \frac{r_o}{r}\right) V_k \qquad (1)$$

where r_o is the inner sphere radius and R is the outer sphere radius. It was also shown that it is possible to correct for the diverging effect of the accelerating lens aperature (A) on the electron rays (positive spherical aberration) by repositioning the point source on the axis a distance p from the innermost spherical electrode of radius a, where

$$p = a\left[1 - \frac{1}{4(1-a/b)}\right]^{-1} \qquad (2)$$

and b is the radius of the outer collector electrode. This will cause a virtual source to appear at the center of symmetry of the spherical system.

In order to check the above calculations a model of the design was placed in an electrolytic tank so equipotential plots could be made. Electron trajectories were plotted by hand using graphical trajectory plotting techniques. The proper position for the cathode to correct for accelerating lens aperature effects in the

design shown in Figure 1 was determined to be .022 inches behind the center of symmetry of the system. With the cathode placed at that position equi-potential plots showed that electron trajectories formed a virtual source at the center of symmetry to a 6^{o} beam half angle. Since the present design limits the actual beam half angle to 1^{o}, the system should not exhibit appreciable spherical aberration. Table I gives the electrode dimensions, aperature sizes and calculated voltage ratios for each electrode in the spherical system.

The most difficult modification made to the system was the substitution of a mesh for the single crystal collector. All of the hemispherical electrodes used in the design were spun from 0.030 inch flat molybdenum stock and lapped to final size and finish. For electrode E a copper insert with a 0.150 inch diameter hole in the center and the same radius of curvature as the molybdenum hemisphere was brazed into the center of the hemisphere. A stainless steel form, lapped with the copper insert to the same radius of curvature and oxidized in wet hydrogen at 800^{o}C. was made. This form was then used to hold a 1000 line per inch (LPI) copper mesh over the hole and form the mesh to the radius of curvature of the electrode while making a gold diffusion braze to attach the mesh to the copper insert. The forming and diffusion braze were made in a vertical hydrogen furnace at 700^{o}C. The copper insert and mesh were then vapor plated with platinum to attempt to avoid the problem of oxide overlayers and patch field which would distrub the local electric potential from its true value.

At the present time the analyzer tube has been assembled and is awaiting evacuation. It is planned to use a <310> oriented tungsten tip in the tube to check operation and resolution.

TABLE I

Electrode	Inner Radius (in.)	Aperture Diameter (in)	Rel. Voltage
A	0.156	0.120	1.0
B	0.415	0.028	0.264
C	0.555	0.028	0.164
D	0.798	0.028	0.060
E	1.196	0.150 (covered by 1000 LPI copper mesh)	0

III THE INFLUENCE OF ADSORBATES ON THE TOTAL ENERGY DISTRIBUTION OF FIELD EMITTED ELECTRONS

One of the motivations for field emission total energy distribution (TED) measurements of adsorbate-coated substrates stems from the possibility that the interaction potential of the adsorbate may alter the transmission probability and, hence, the TED. This expectation has been given a theoretical basis by Duke and Alferieff[1] (D and A), who treated field emission through adsorbed atoms by an atomistic one-dimensional pseudo-potential model. In the case of metallic adsorption, their results predict an increase in transmission apart from the usual work function lowering. This approach is in contrast to other treatments which assume the adsorbed layer modifies the Fowler-Nordheim equation either through the work function term[2,3] or the image potential term.[4] In each of these cases including the D and A theory a change in both the preexponential and exponential terms of the Fowler-Nordheim (FN) equation is predicted. The D and A theory is unique in the case of metallic adsorption since it also predicts additional structure in the TED curve when the valence level of the adsorbate falls below the substrate Fermi level.

Recent experimental results have shown the FN theory to be inadequate for describing the TED from the <100> directions of clean molybdenum[5] and tungsten[6] due to band splitting near the Fermi level. All other major crystallographic directions of both molybdenum and tungsten show no gross deviations from the Sommerfeld model, upon which the FN theory is based, in spite of the non-free-electron nature of the metals. The somewhat surprising success of the Sommerfeld model in describing field emission from the transition metals is the result of the narrow energy band ($\sim$0.2 eV) sampled by field emission. Accordingly, the specific effects of the emitter band structure are visible only when unusually small Fermi surfaces are emitting[7,8] or when band gaps occur within $\sim$0.2 eV of the Fermi level.

Historically the FN theory has been utilized with apparent success to describe the field emission characteristics of both clean and adsorbate

coated surfaces. Recent use of probe techniques, which confine work function and energy distribution measurements to single atomically smooth crystal faces, has eliminated the undesirable averaging and allows a more stringent test of the FN theory. The evidence that work function changes due to adsorption are also reliably given by the FN equation is now substantial.

At present, two minor modifications to field emission calculated work functions of adsorbed layers have been considered. The first is due to Gomer[2], who considered the detail shape of the contact potential within the adsorbed layer and its effect on the FN equation. The graphical method employed by Gomer showed its effect on the FN equation. The graphical method employed by Gomer showed that the apparent contact potentials obtained from FN analysis are lower than actual due to the discreet nature of the dipole potentials of the adsorbed atoms. This correction, which increases linearly with field becomes of significant consequence only at coverages less than 0.1 monolayer and field strength in excess of 3×10^7 V/cm.

The second correction to field emission work function calculations stems from the polarization of the adsorbate due to the applied electric field. This correction has now been substantiated in a number of cases[9,10,11] and has successfully explained the variation of emitting area upon adsorption. This effect, which increases the work function ϕ, is linear with electric field F and thereby in first order appears as an alteration to the preexponential term of the FN equation 5 such that the ratio of the adsorbate coated emitting area A to the clean emitting area A_o is given by:

$$\log A/A_o = -4.20 \times 10^7 \, \phi^{1/2} \, g \, \pi \sigma \, \alpha/\epsilon \qquad (3)$$

where α is the adsorbate polarizability in cm^3, σ the adsorbate density in atoms/cm^2, g a factor ranging from 2 to 4 (depending upon the degree of localization of the induced dipole to the adsorbate), and ϵ is the ratio of the applied to actual field at the adsorbate F/F_o. One approximation of ϵ comes from the Topping[12] model in which the value of ϵ is given by $\epsilon = 1 + 9 \, \alpha \, \sigma^{3/2}$ and represents the

reduction in field at a specified adsorption site due to the accumulated effect of the field induced dipoles in a square array of adsorbed particles. Experimental values of the preexponential changes in the FN equation for both electropositive[12] and electronegative[9,11] adsorbates have given reasonable values of a calculated in terms of equation (3). An additional modification of the FN equation has been given by van Oostrom,[4] who considered the alteration of the image potential term by the adsorbate. In this case the adsorbate was treated as a structureless dielectric film of finite thickness which modified the image potential. This modification, which is in the same spirit as the first correction mentioned above, appears to be valid only for multilayer adsorption.

The above mentioned modifications to the FN theory due to adsorption do not predict changes in the TED which cannot be accounted for by corresponding changes in F and/or $\emptyset$. Such is not the case for the D and A one-dimensional pseudo-potential model of field emission. In this novel treatment of the effect of adsorbed layers on field emission, it is shown that the adsorbed particle is able to affect resonance tunnelling of the electrons when the valence level of the adsorbed particle is properly oriented with respect to the Fermi level. Under certain conditions of metallic adsorption additional structure in the TED is predicted along with large enhancements ($10\text{-}10^4$) in the preexponential term of the FN equation.

It thus should be possible to examine the reliability of the various modifications to the FN theory by simultaneous analysis of the FN equation and TED. In this study we have examined cesium and barium adsorption on a few crystal planes of molybdenum and tungsten with respect to their effect on the TED and current-voltage relationships throughout the monolayer coverage.

EXPERIMENTAL APPROACH

Before proceeding it will be helpful to list the relevant equations pertinent to the current voltage I(V) characteristics of field emitted electrons and the TED. For the Sommerfeld model, upon which the FN theory of

field emission is based, the current density per unit total energy $J(\epsilon)$ (where ϵ is the energy E relative to the Fermi energy E_f) is given by:[13]

$$J(\epsilon) = J_o \, e^{\epsilon/d} \, /d \, (1 + e^{\epsilon/pd}), \tag{4}$$

where $p = kT/d$ and J_o, the total current density (integrated over all ϵ) at 0^oK, is given by:[14]

$$J_o = \frac{1.54 \times 10^6 \, F^2}{\phi \, t^2 \, (y)} \exp \left[-6.83 \times 10^7 \, \phi^{3/2} \, v \, (y) \, / \, F \right] . \tag{5}$$

(The numerical form assumes J_o in A/cm^2, F in V/cm and ϕ in eV). The expression for the parameter d is

$$d = 9.76 \times 10^{-9} \, F/\phi^{1/2} \, t \, (y) \, (eV). \tag{6}$$

The image correction terms t(y) and v(y) are slowly varying tabulated functions[14] of the auxiliary variable $y = (e^3 \, F)^{1/2} \, /\phi$. If the condition $\epsilon/pd < 0$ is met equation (4)can be expressed as

$$J(\epsilon) \cong J_o \, e^{\epsilon/d} \, /d \tag{7}$$

In a retarding potential analyzer we note that ϵ can be related to the collector work function ϕ_c and the emitter-to-collector bias potential V_t in the form $\epsilon = \phi_c - V_t$, thereby allowing equation (7) to be written in the working form

$$\log J(\epsilon) = \log \frac{J_o}{d} + (\phi - V_t) / \, 2.3d \tag{8}$$

Thus, the value of d can be obtained from the slope $m_e = 1/2.3d$ of a plot of $\log J(\epsilon)$ versus V_t. Experimental values of $J(\epsilon)$ can be evaluated from the first derivative of the collector current I_c with respect to V_t

$$J(\epsilon) = - \, n \, dI_c/dV_t, \tag{9}$$

where n is an arbitrary constant of normalization.

It is further observed that a "Fowler-Nordheim" plot of $\log I_o/V^2$ versus $1/V$ yields a slope m_f which is related to the emitter work function ϕ_f and the geometric factor $\beta = F/V$ as follows:

$$m_f = -2.96 \times 10^7 \, \phi_f^{3/2} \, s(y)/\beta \ (\text{cm}), \tag{10}$$

where $s(y) = 0.943$ over the range of y encountered in practice. The value ϕ_f relative to a reference value $\bar{\phi}$ can be readily established as shown by rewriting equation (10) as follows:

$$\phi_f = \bar{\phi} \, (m_f/m_o)^{2/3}, \tag{11}$$

where m_o is the FN plot slope for the reference work function (usually the surface average) and the value β is assumed unchanged. Because of the difficulty in determining accurate values of ϕ and β, equation (10) cannot be employed for precise work function calculation; however, as pointed out by Young[15], the expressions for m_e and m_f can be combined to give

$$\phi_e = -3m_f \, t(y)/2 \, m_e \, V \, s(y), \tag{12}$$

where V is the anode voltage. Accordingly, within the framework of the Sommerfeld model a value of work function can be ascertained from combined energy distribution and FN plots from equation (12) which eliminates assumptions concerning $\bar{\phi}$ and β.

It will be our purpose to examine various experimental parameters obtained from TED and FN plots for self-consistency as a function of adsorbate coverage and attempt to interpret the results in terms of the theoretical modifications discussed in the preceeding section.

EXPERIMENTAL PROCEDURE

The experimental energy analyzer tube and procedure have been described previously.[6] Briefly, the tube designed by van Oostrom,[4] is a

retarding potential analyzer equipped with magnetic deflection to align emission from a particular direction with a small aperture in the anode plate. Without magnetic deflection the analyzer tube gave a resolution of 15 to 20 mV. Both molybdenum and tungsten substrates were employed in this investigation. Attention was mainly given to those planes perpendicular to the wire axis owing to the slight alteration of the TED when magnetic deflection was employed. Zone melted single crystal wire was employed to fabricate emitters with the desired crystal direction along the wire axis.

The approximate geometric emitting area seen by the 1 mm diameter probe hole was approximately $3.4 \times 10^{-4} r^2$ (cm^2), where r is the emitter radius. For emitter radii of 1 to 2×10^{-5} cm employed in this study the emitting area was the order of 3 to 13×10^{-14} cm^2; this corresponds to approximately 30 to 130 substrate atoms contributing to the probe emission from a (100) plane.

Deposition of cesium onto the substrate was accomplished by resistively heating to 1100° K a small bead of cesium zeolite fused onto a platinum wire. This method has proven to give a pure flux of cesium ions which can be focused onto the emitter. The barium source consisted of a short segment of iron clad barium wire mounted on Nichrome leads for resistive heating. A four lead tungsten loop supporting the emitter was utilized for heating the emitter to known temperatures. The results reported here were obtained at 77° K; this was accomplished by immersing the entire analyzer tube in a liquid nitrogen cryostat.

RESULTS

The results of basic significance to this study are (1) the agreement of the TED shapes with equation (4), throughout the coverage range, (2) the variation of A/A_o with adsorbate coverage and (3) the agreement between ϕ_f and ϕ_e as calculated by equations (11) and (12) respectively. The emitting areas are calculated both from the value of the intercepts of the FN plots

and from FN slope data alone by a method described elsewhere.[16] Both methods yielded nearly identical A values in this investigation. Our method of analysis was therefore to treat the data according to the FN theory in a self-consistent manner and examine any discrepancies with respect to existing modifications of the FN theory for adsorption.

In obtaining values of ϕ_f via equation (11) for various planes or as a function of coverage it should be emphasized that a uniform field factor β is assumed. Thus, within the framework of the FN model disagreement between ϕ_f and ϕ_e can only be attributed to a difference between the local β_c and the average $\bar{\beta}$ field factors. The apparent change in β can be obtained from the relation $(\phi_e/\phi_f)^{3/2} = \beta_c/\bar{\beta}$.

Figures 2 to 8 show representative TED curves for the various systems investigated along with the theoretical curves derived from the value of d (and hence p) obtained from the best fit slope m_e of the low energy tail. The normalization constant n of equation (9) was adjusted to allow overlap in the latter region. The poor fit on the leading edge and near the peak is due to the limitations imposed by the analyzer resolution. A somewhat disturbing deviation from theory at low values of dI_c/dV_t on the low energy side of some of the experimental TED data is believed to be caused by an artifact of the analyzer and should be ignored. The values of dI_c/dV_t were obtained by monitoring the change in I_c for a 10 mV increment in V_t. Values of σ for the Cs/W, Cs/Mo and the Ba/Mo systems were obtained from previously established relationships between ϕ and σ [17,18].

Barium on (111) Mo

The TED curves for barium on (111) Mo give a reasonably good fit to equation (4) as observed in Figures 2-4. We observe no anomalous humps or shape changes throughout the coverage range that cannot be described by the equation (2) parameters. On the other hand, Figure 9 shows that the apparent value of $\beta_c/\bar{\beta}$ is not constant, but is first larger and then smaller than unity as the coverage increases. The length of the vertical bars are

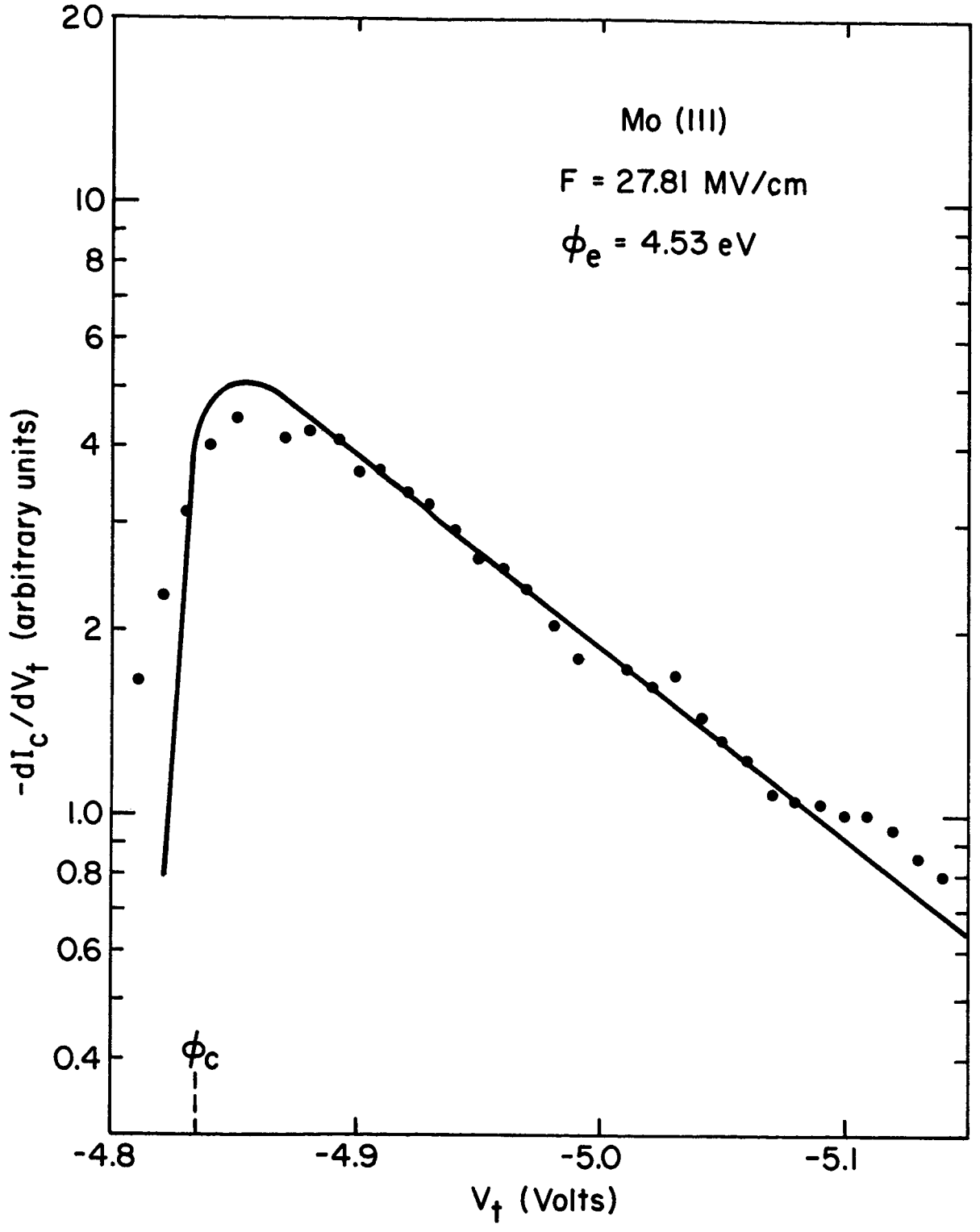

Figure 2. Solid curve is derived from equation (2) for p = 0.048. Data points are experimental values of the TED for clean (111) Mo.

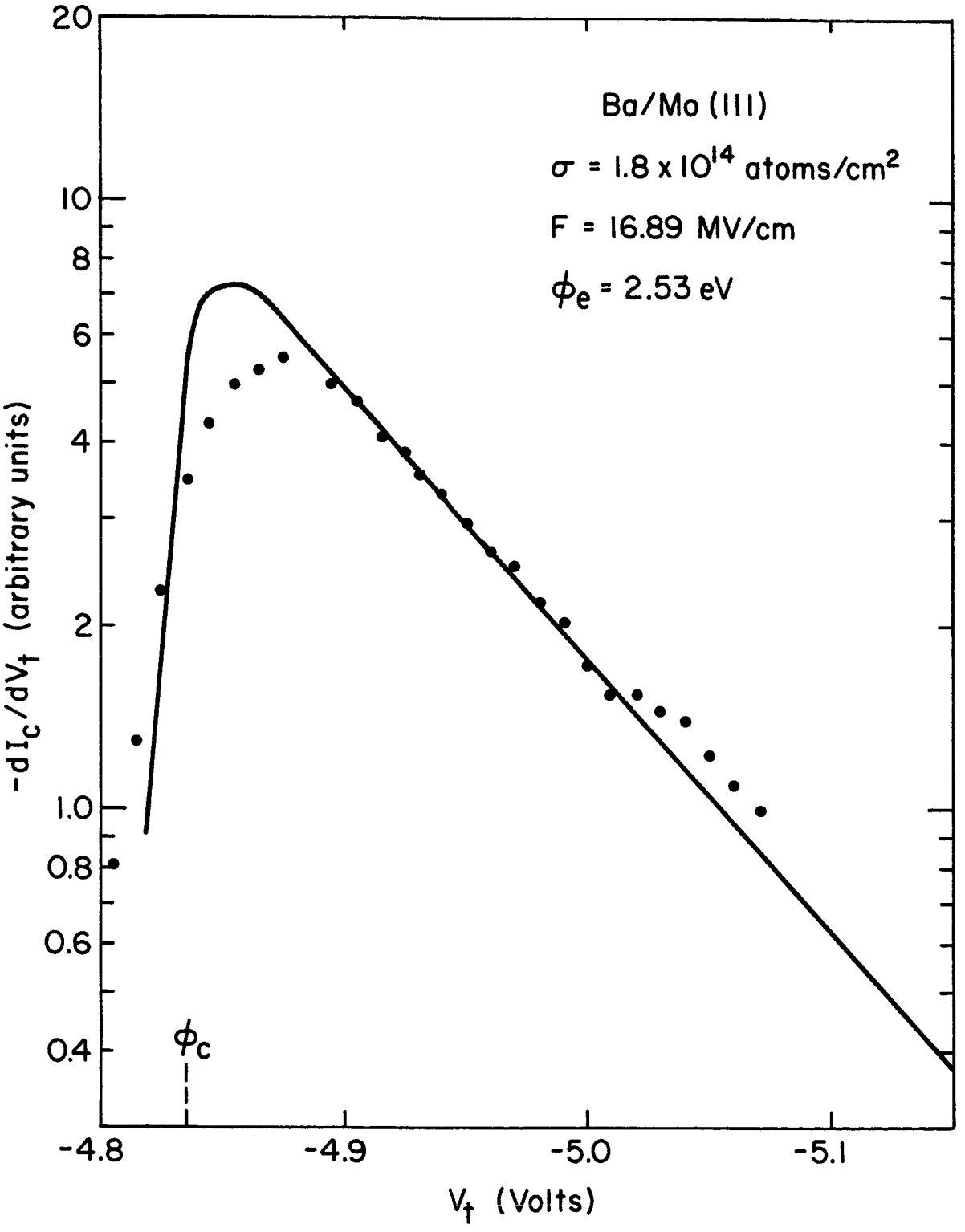

Figure 3. Solid curve is derived from equation (2) for p = 0.068. Data points are experimental values of the TED for barium on (111) Mo.

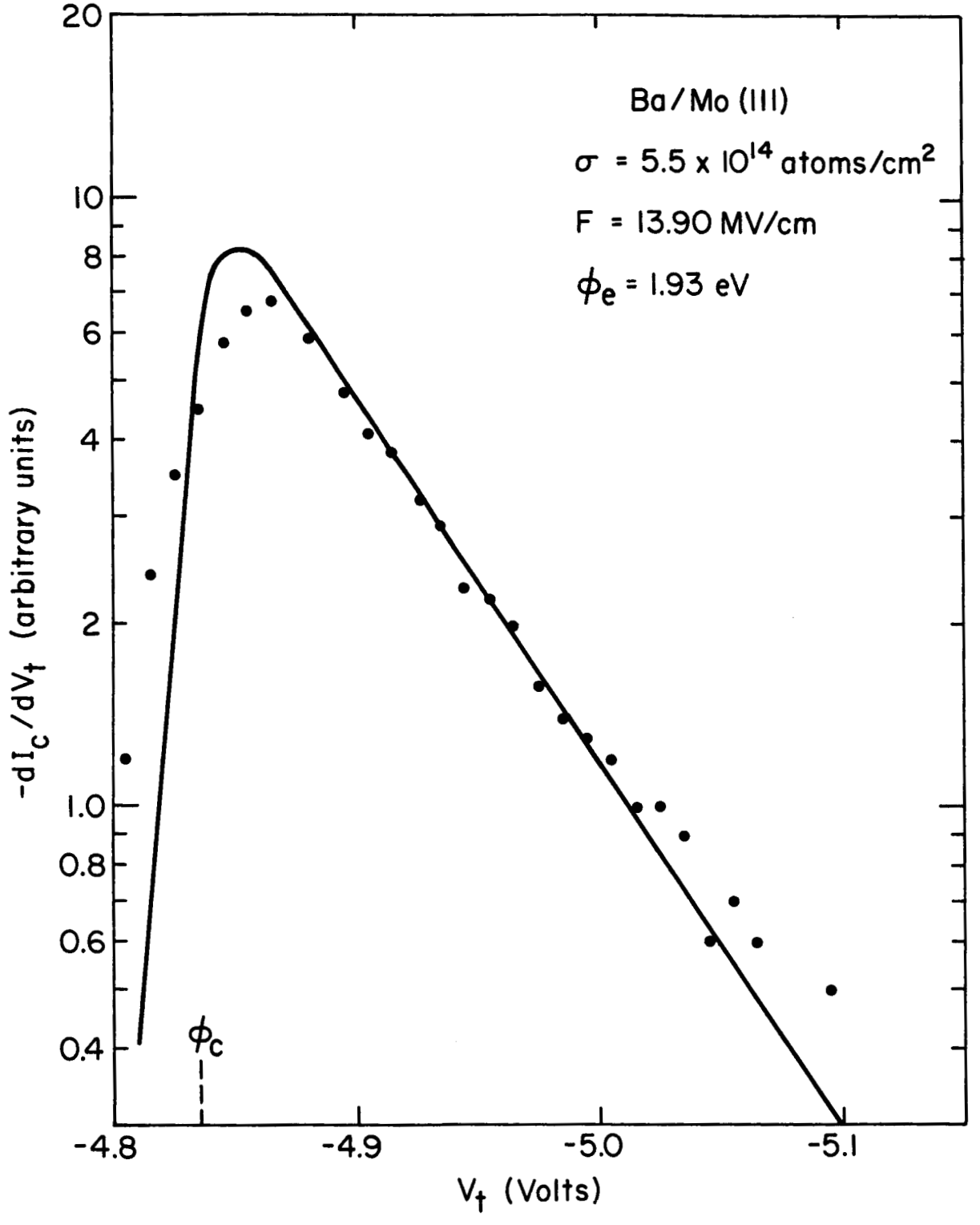

Figure 4. Solid curve is derived from equation (2) for p = 0.091. Data points are experimental values of the TED for barium on (111) Mo.

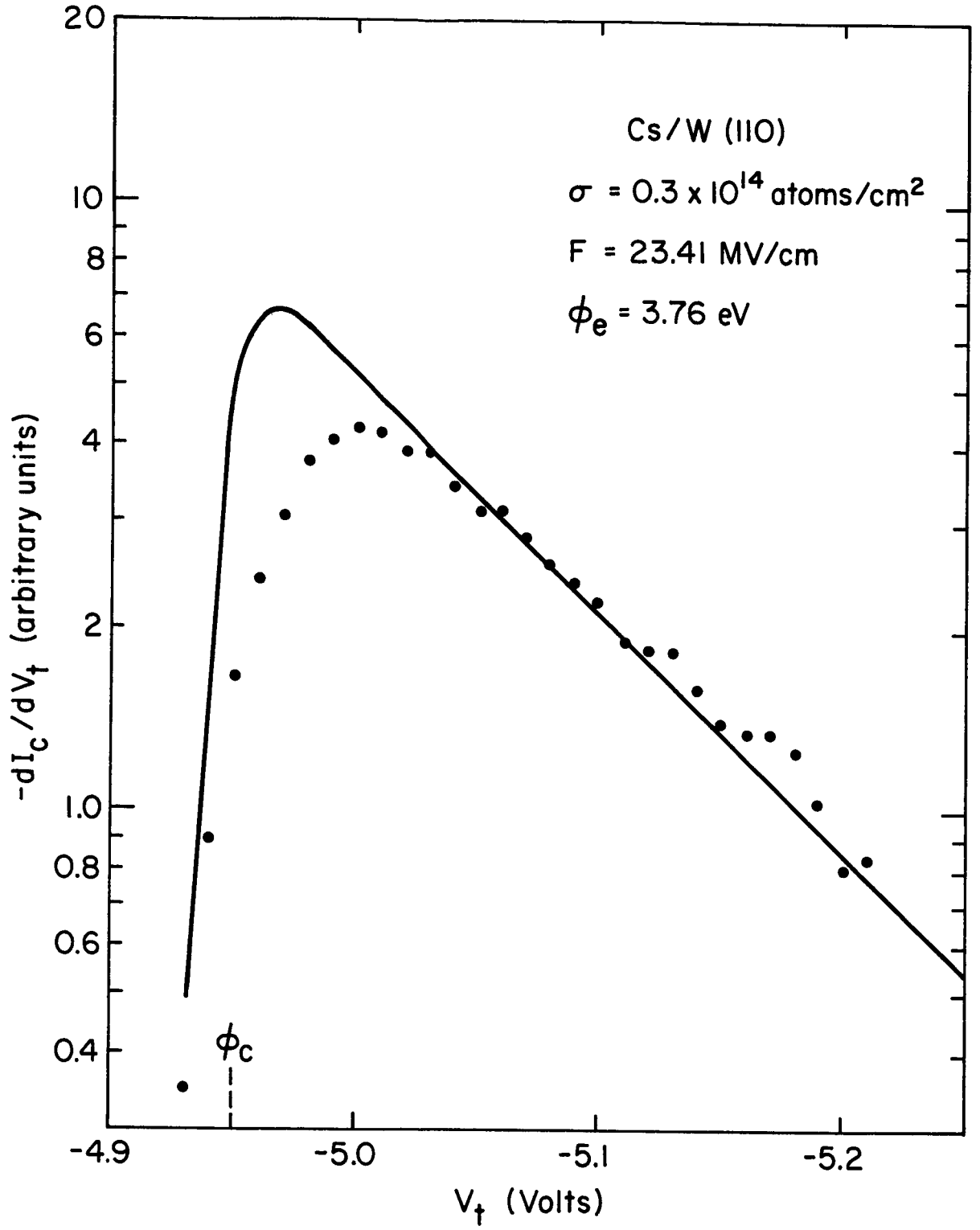

Figure 5. Solid curve is derived from equation (2) for p = 0.060. Data points are experimental values of the TED for cesium on (110) W.

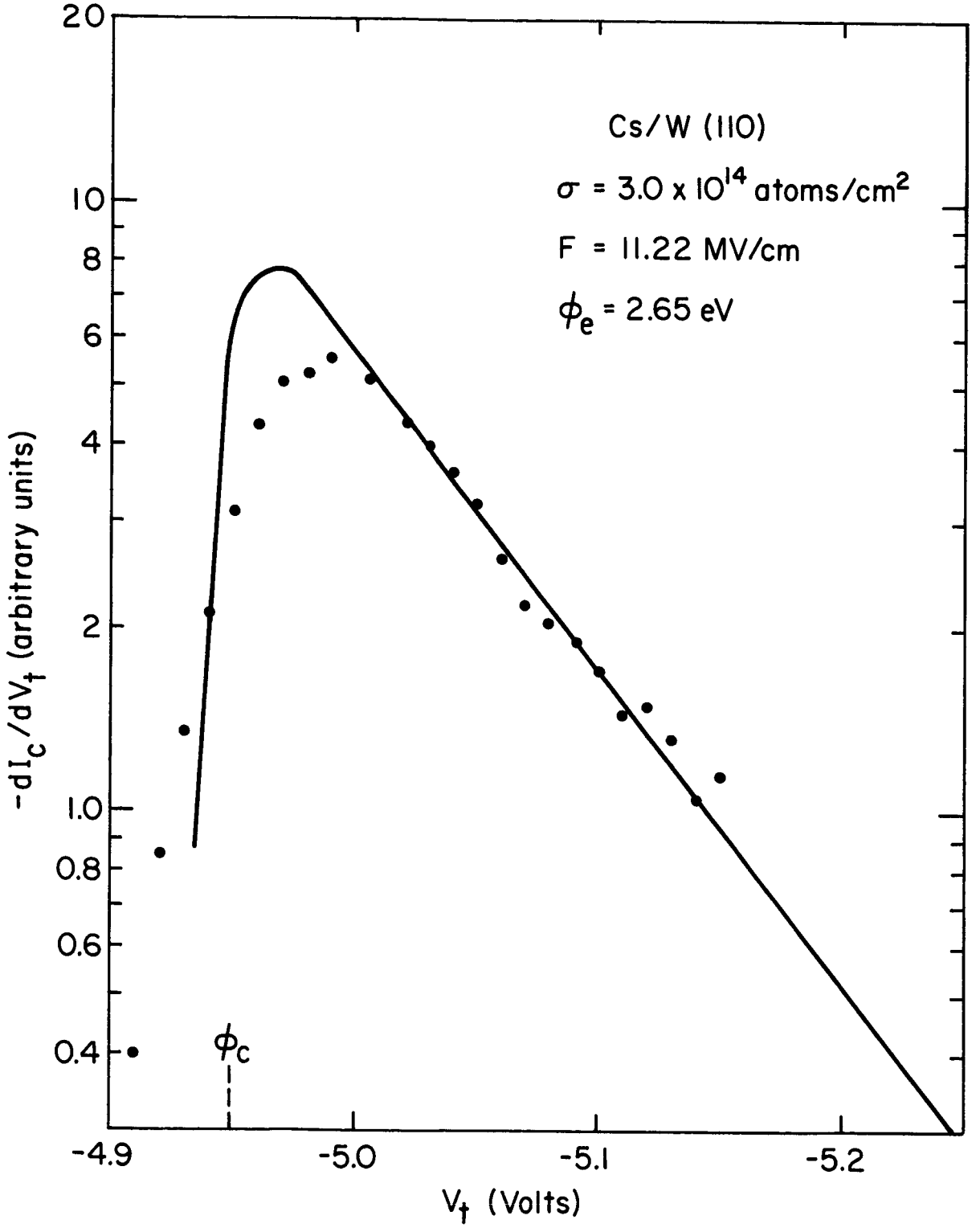

Figure 6. Solid curve is derived from equation (2) for p = 0.079. Data points are experimental values of the TED for cesium on (110) W.

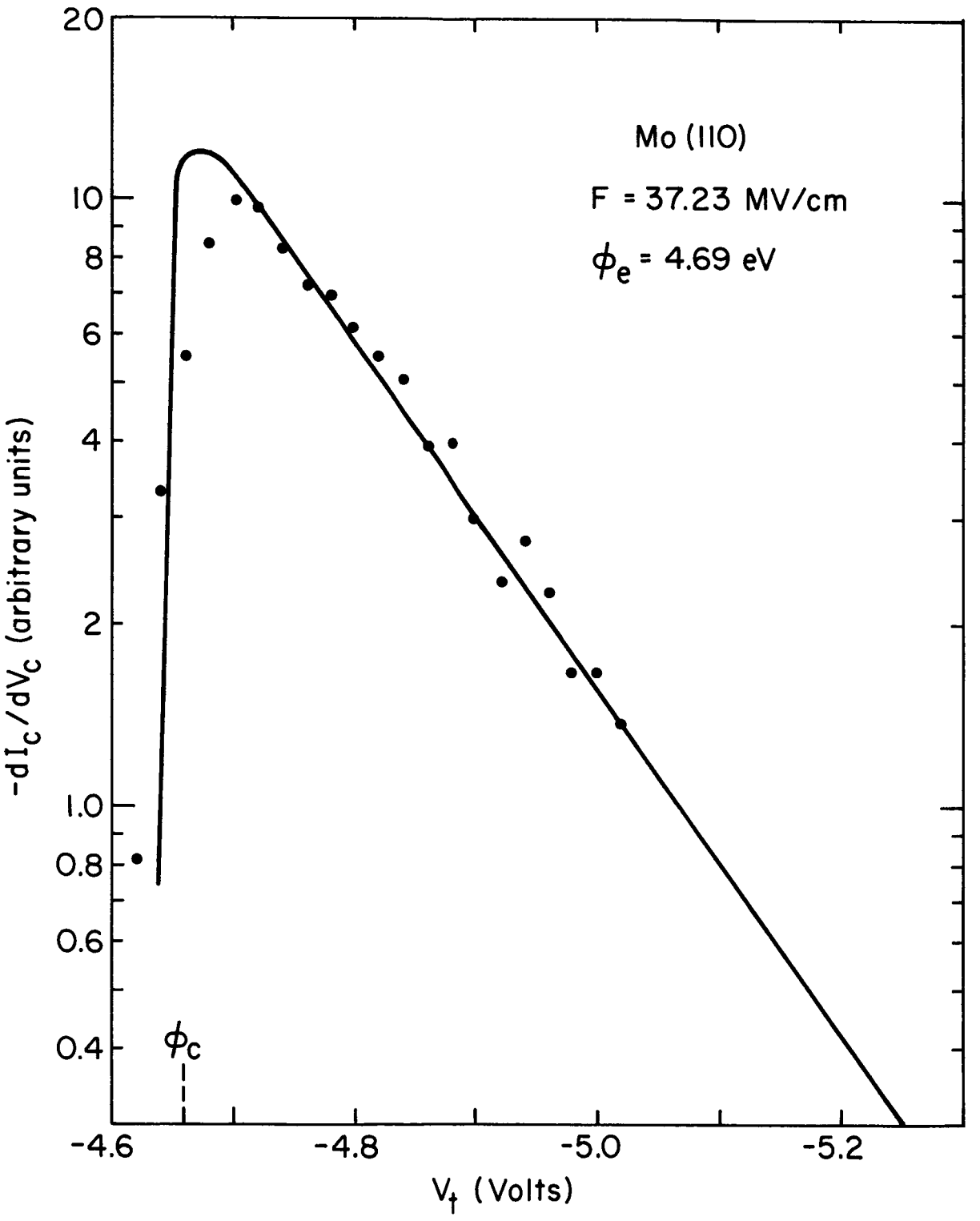

Figure 7. Solid curve is derived from equation (2) for p = 0.044. Data points are experimental values of the TED for clean (110) Mo.

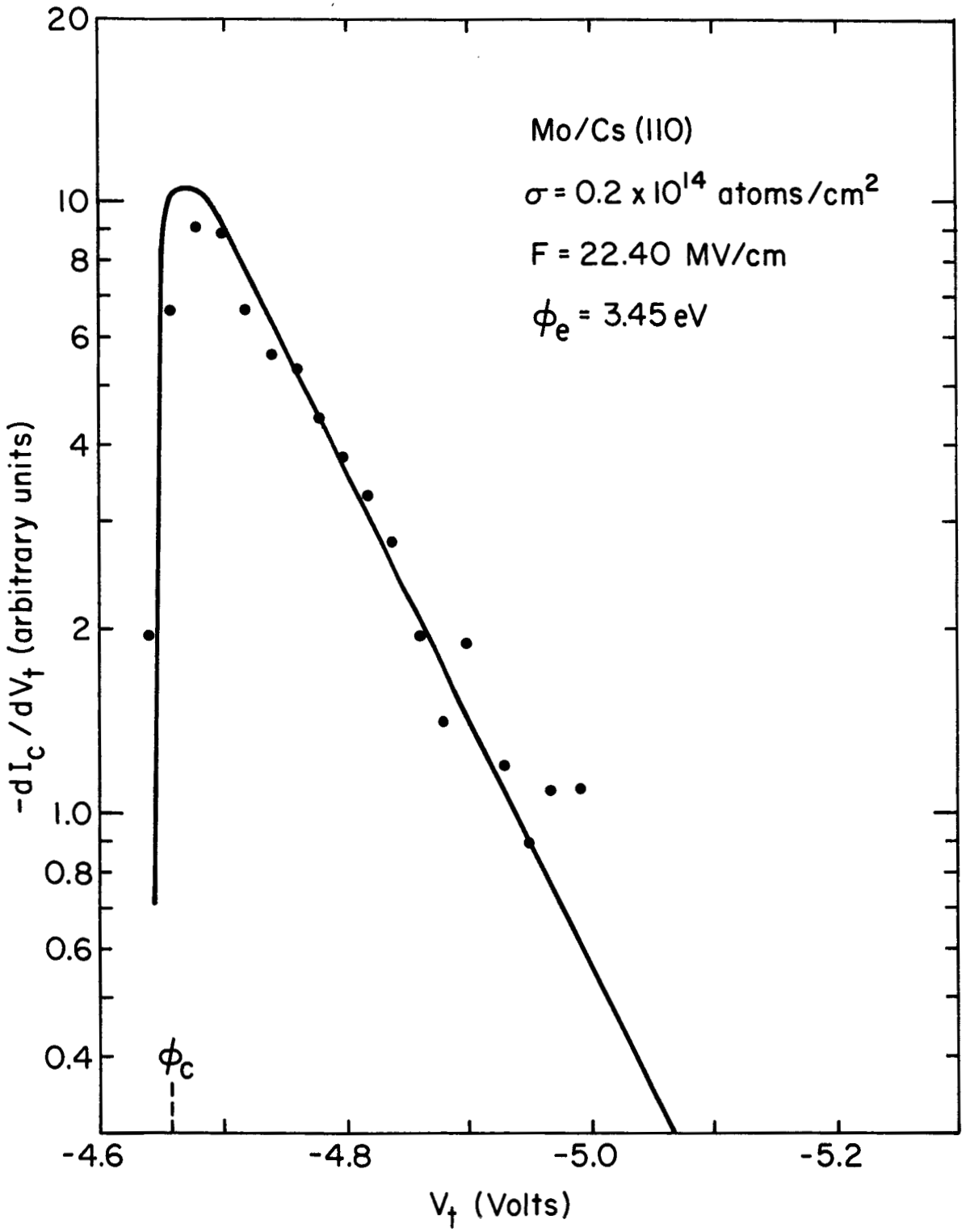

Figure 8. Solid curve is derived from equation (2) for p = 0.062. Data points are experimental values of the TED for cesium on (110) Mo.

the extreme values of $\beta_c/\bar{\beta}$ determined at different field strengths and probably represents the uncertainty in experimental values of m_e, since no systematic variation with field strength is observed in these results. Adherence to the FN model yields a local field enhancement $\beta_c/\bar{\beta}$ at $\sigma = 0$ of 14%, $\phi_c = 4.53$ eV and $\phi_f = 4.15$ eV. Several measurements in this laboratory have yielded the somewhat high value of $\phi_e = 4.5 \pm 0.1$ eV for the (111) plane of Mo.

In addition to the variation of $\beta_c/\bar{\beta}$ with σ, the Figure 9 results also show a significant reduction in the apparent emitting area A/A_o which goes through a slight minimum with increasing σ. It is interesting to note that this minimum in A/A_o occurs near the minimum in the ϕ_f versus σ curve.

Cesium on (100) and (110) W

Representative plots of the TED data for cesium on (110) W shown in Figures 5 and 6 also indicate a reasonably good fit to the theoretical expression given in equation (4) and show no anomalies in their shape with increasing cesium coverage. In contrast to the barium results, $\beta_c/\bar{\beta}$ increases significantly above unity in the midcoverage range as observed in Figure 10. As noted previously,[6] the occurrence of a value $\beta_c/\bar{\beta} > 1$ for the clean (110) plane is physically unacceptable for this highly faceted region. We therefore suspect some inadequacy of the Sommerfeld model for emission from the clean <110> direction of W. Also, in contrast to the Ba/Mo results, A/A_o values for both the (110) and (100) planes are larger than unity at low coverages.

Cesium on (110) Mo

Results for cesium on (110) Mo have been limited to the low coverage region and are shown in Figure 11. The Mo results show a value of $\beta_c/\bar{\beta} \simeq 1$ for $\sigma < 0.3 \times 10^{14}$ atoms/cm^2, in agreement with the (110) W data. Also in agreement with both the previously discussed systems, the TED data agrees reasonably well with equation (4) in the limited range of σ investigated.

The most striking contrast with the (110) W results is the much

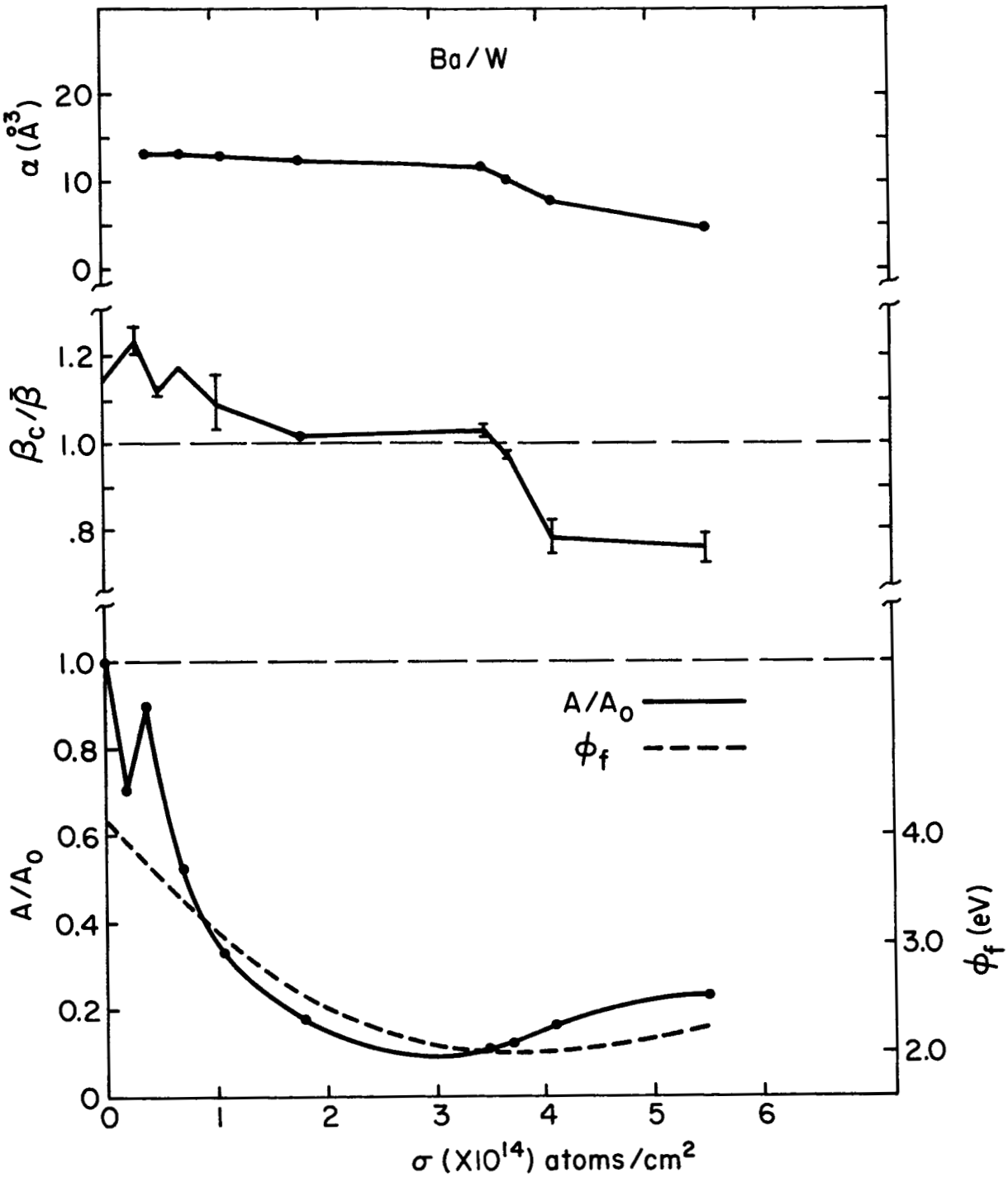

Figure 9. The lower curves show the variation of the ratio of the adsorbate coated A to clean A_o emitting area and work function ϕ_f with coverage σ. The middle curve gives the ratio $(\phi_e/\phi_f)^{3/2} = \beta_c/\bar{\beta}$ at various coverages. The upper curve shows the variation of polarizability α calculated according to equation (1). These data were obtained from barium on (111) Mo where monolayer coverage occurs near $\sigma = 4.5 \times 10^{14}$.

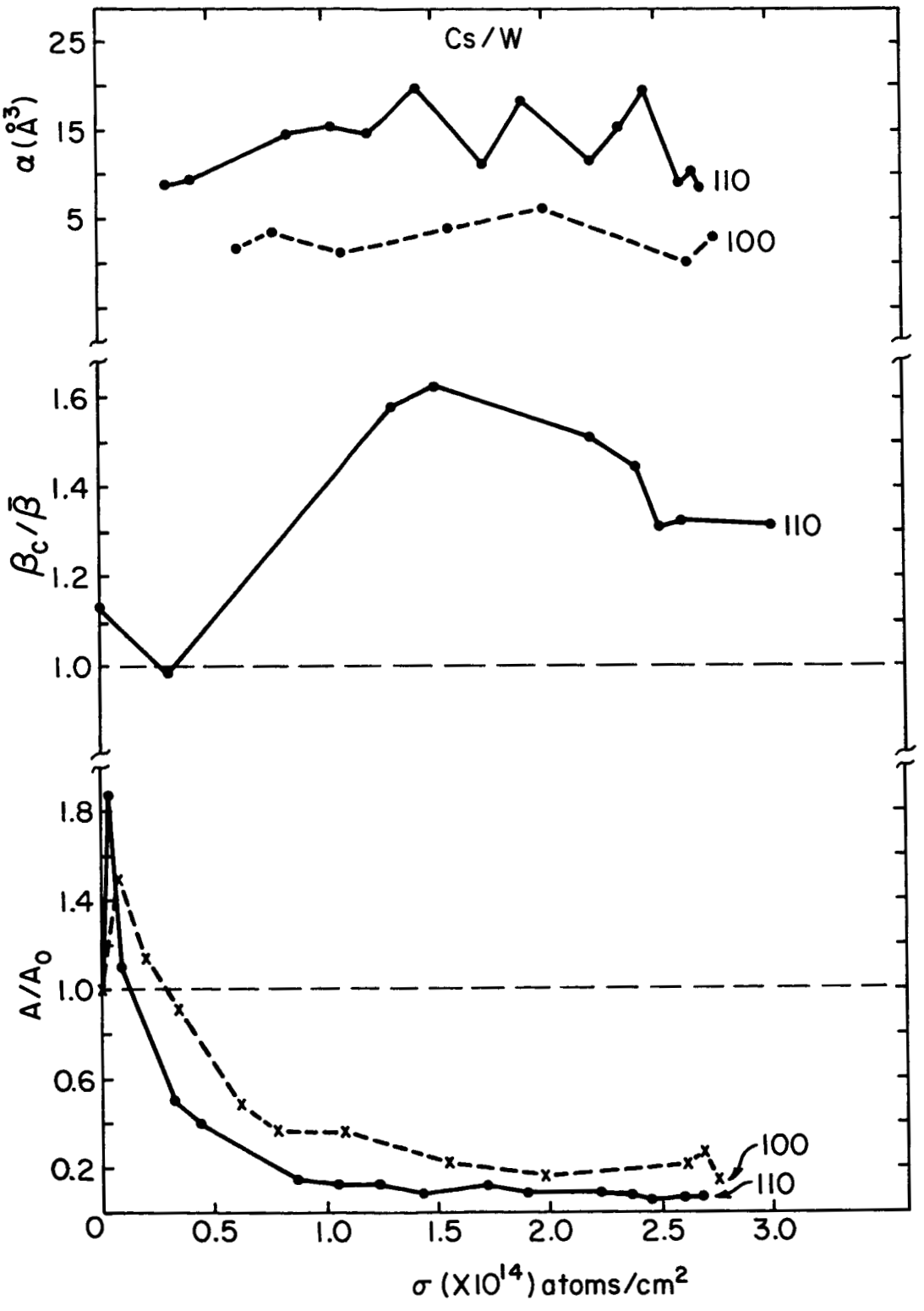

Figure 10. The lower curves show the variation of the ratio of the adsorbate coated A to clean A_o emitting area with coverage σ. The middle curve gives the ratio $(\phi_e/\phi_f)^{3/2} = \beta_c/\bar{\beta}$ at various coverages. The upper set of curves show the variation of α calculated according to equation (1). These data were obtained from cesium on (100) and (110) W where monolayer coverage occurs near $\sigma = 2.7 \times 10^{14}$.

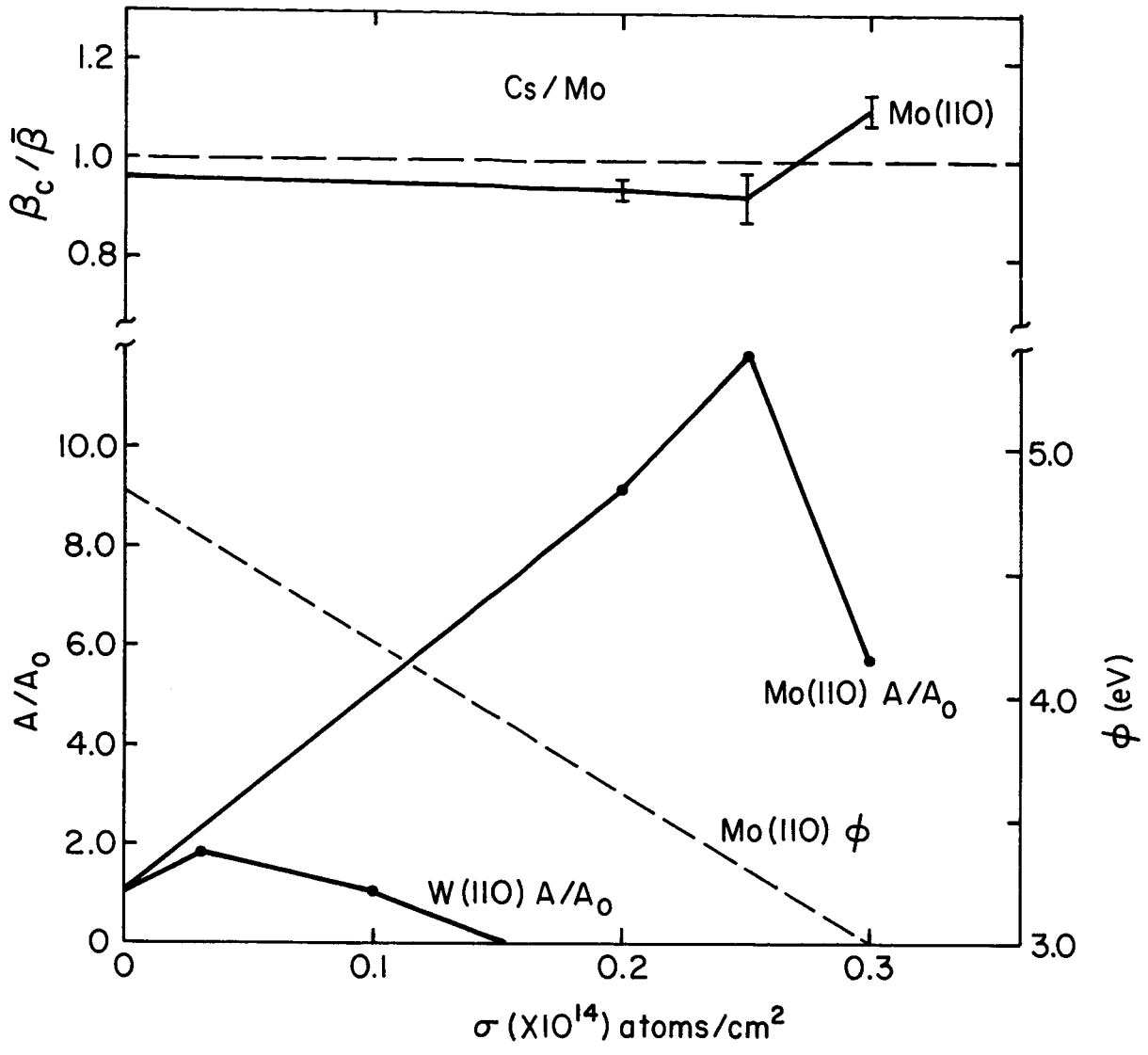

Figure 11. The lower curves show the variation of the ratio of the adsorbate coated A to clean A_o emitting area and work function with coverage σ. The upper curve gives the ratio $(\phi_e/\phi_f)^{3/2} = \beta_c/\bar{\beta}$ at various coverages. These data were obtained from cesium on (110) Mo. The value of A/A_o for (110) W is given for comparison purposes.

larger increase in A/A_o for (110) Mo at low cesium coverage. It should be pointed out that the value of $A_o = 1 \times 10^{14}$ atoms/cm^2 is considerably smaller than the (110) W value of 46×10^{14} atoms/cm,^{2} in spite of the fact that both emitters possessed almost identical radii. Within the framework of the FN theory the small value of A_o can only be explained by a large local magnification; however, this explanation is undesirable in view of $\beta_c/\bar{\beta} < 1$. This raises suspicion that the FN preexponential term may not fully describe clean (110) Mo emission as in the case of (110) W.

DISCUSSION

From these preliminary results one may make several observations regarding the adequacy of the FN model in its original and modified forms to describe metallic adsorption. First, in each of the systems investigated the apparent emitting area seen by the probe varied substantially with adsorbate coverage--a result not explained by the unmodified FN theory. The polarization correction described by equation (3) predicts a decrease in A/A_o with increasing value of $\phi^{1/2}\sigma$ and has been employed to evaluate an effective value of a for the adsorbed particles. Excluding the values of $A/A_o > 1$ at low cesium coverage which clearly cannot be rationalized by the polarization model, we have evaluated the apparent a throughout the monolayer coverage where $A/A_o < 1$ and give the results in Figures 10 and 11. In spite of the classical and phenomenological nature of the polarization correction, it yields a reasonable and constant value of a throughout most of the monolayer coverage for barium and cesium. The values of A/A_o which occur for cesium on (110) Mo, (100) and (110) W at < 0.1 monolayer may be attributed to a resonance tunnelling enhancement of the emission as described by D and A. Inasmuch as cesium at low coverage on the (100) and (110) planes of W and the (110) plane of Mo give a negative value for the difference between the adsorbate ionization potential V_i and work function $V_i - \phi$ one expects a small increase in coverage to align the broadened valence level of the adsorbate with the substrate Fermi level. It is under the latter conditions that maximum

resonance tunnelling, manifested by an enhanced apparent emitting area and structure in the TED, is expected.[1] With increasing coverage $V_i - \phi$ becomes larger (in a positive sense) and resonance tunnelling diminishes due to a decrease in the interaction between the tunnelling electrons and the adsorbate valence band. The conspicuous absence of values $A/A_o > 1$ for barium on (111) Mo can be attributed to the larger positive value of $V_i - \phi \simeq 1$ eV at zero coverage which positions the adsorbate valence level below the substrate Fermi level, thereby reducing adsorbate-induced resonance tunnelling.

One may speculate further that becuase $V_i - \phi = -0.94$ for cesium on (110) Mo, as opposed to -1.95 for cesium on (110) W, the valence level of the former is more favorably aligned with the substrate Fermi level at low coverage. This may account for the much larger values of A/A_o for (110) Mo. Further examination of the unusually small value of A_o for Mo should be performed before firm conclusions based on detailed comparison of the relative magnitudes of the A/A_o values should be made.

Although possible meanings of the variation in $\beta_c/\bar{\beta}$ with adsorbate coverage are manifold, it is basicallya measure of the self-consistency between the energy spectrum description of field emission as given in equation (4) and the I (V) relationship given in equation (5). Specifically, within the framework of the FN model β is a geometrical factor which can be influenced by atomic sized perturbations as demonstrated in the field ion microscope. In this sense, large adsorbates such as cesium on a smooth (110) plane of W or Mo should cause an increase in $\beta_c/\bar{\beta}$, particularly if clustering occurs; $\beta_c/\bar{\beta}$ should then decrease as a smooth monolayer is formed. By the same token an atomically rough plane, such as a (111), may not exhibit such an increase in $\beta_c/\bar{\beta}$, but rather a decrease if the surface of the overlayer is geometrically smoother. Such is apparently the case if one compares the gross features of the variation in $\beta_c/\bar{\beta}$ with σ for barium on (111) Mo and cesium on (110) W. It is unlikely that geometric effects alone can account for the exceptionally large values of $\beta_c/\bar{\beta}$ in the midcoverage range of cesium on (110) W.

At this point it is important to emphasize that $\beta_c/\bar{\beta}$ is proportional to $1/m_e^{3/2}$, thus an increase in m_e due to other effects should cause a reduction in $\beta_c/\bar{\beta}$. According to the D and A theory,[1] resonance tunnelling effects for adsorbed atoms whose valence level is aligned below the Fermi level are manifested in the TED curves by larger values of m_e. This effect would assert itself in our results as a diminution in $\beta_c/\bar{\beta}$ and may be a contributing cause to the low and constant values for $\beta_c/\bar{\beta}$ at low cesium coverages on the (110) plane of Mo and W where previously mentioned increase in A/A_o occurs.

It is noteworthy that in spite of these results which give some measure of support to resonance tunnelling at small or negative values of $V_i - \emptyset$, we find no apparent field dependent structure in the TED curves in the corresponding coverage interval as predicted by D and A. Rather, analysis of the Table II to IV tabulations of the data show $m_e \propto 1/F$ in general agreement with the FN model.

CONCLUSIONS

The results of this investigation which are preliminary in nature provide a measure of support for adsorbate induced resonance tunnelling. Primarily this support comes from the increase in the apparent emitting area, since the additional prediction of structure in the TED curve was not observed. The experimental evidence supporting resonance tunnelling occurs only when $V_i - \emptyset$ is near zero, as expected. Over the major portion of the monolayer region the variation in apparent emitting area and can be described by the field polarization model. From this study it is apparent that field emission TED and I(V) measurements of appropriate surfaces may be potentially useful in shedding light on the nature of adsorbate bonding modes. However, additional investigations of the TED of field emitted electrons for other systems are necessary before a clear picture of the relative importance of the various modifications to the FN theory due to adsorbed layers can be clearly established.

Table II. Results from Ba/Mo (111) where $\bar{\beta} = 1.334 \times 10^{4}$ cm^{-1}

σ ($\times 10^{14}$) atoms/cm^2	m_f volts	m_e volts^{-1}	V volts	A ($\times 10^{-14}$) cm^2	ϕ_f eV	ϕ_e eV
5.5	7141	1.265	823	6.29	2.25	1.83
5.5	7141	1.679	1042	6.41	2.25	1.93
4.1	6201	1.219	755	4.61	2.04	1.68
4.1	6201	1.564	915	4.69	2.04	1.80
3.7	5973	1.518	779	3.36	1.99	1.95
3.7	5973	1.748	891	3.40	1.99	1.97
3.5	6217	2.093	731	3.06	2.10	2.11
3.5	6217	1.794	915	3.11	2.05	2.07
1.8	8476	1.863	1042	5.11	2.52	2.93
1.8	8476	2.231	1267	5.18	2.52	2.53
1.05	11270	2.162	1285	9.20	3.05	3.15
1.05	11270	2.921	1644	9.36	3.05	3.37
0.7	13740	2.645	1553	15.2	3.48	3.87
0.7	13740	2.650	1949	15.4	3.48	3.12
0.5	15830	2.921	1840	25.12	3.82	4.16
0.3	17270	3.243	1949	19.60	4.05	4.75
0.3	17270	3.703	2330	19.80	4.05	4.58
0	17910	3.174	2085	28.09	4.15	4.53

Table III. Results from Cs/W (110) where $\bar{\beta} = 2.022 \times 10^{4}$ cm^{-1}

σ ($\times 10^{14}$) atoms/cm^2	m_f volts	m_e volts^{-1}	V volts	A ($\times 10^{-14}$) cm^2	ϕ_f eV	ϕ_e eV
0	19610	3.910	999	46.0	5.82	6.32
3.0	4620	1.932	555	3.7	2.22	2.67
2.6	4100	1.748	484	0.98	2.05	2.47
2.5	3850	1.771	484	1.3	1.96	2.35
2.4	3490	1.587	393	4.4	1.84	2.35
2.2	3010	1.610	368	4.9	1.67	2.20
1.5	2630	1.541	322	4.9	1.52	2.11
1.3	3190	1.725	393	6.6	1.73	2.35
0.3	10310	2.760	1158	42.0	3.79	3.75

Table IV. Results from Cs/Mo (110) where $\bar{\beta} = 2.01 \times 10^{4}$ cm^{-1}

(x 10^{14}) atoms/cm^2	m_f volts	m_e volts^{-1}	V volts	A (x 10^{-14}) cm^2	ϕ_f eV	ϕ_e eV
0.20	9174	3.731	1117	10.0	3.56	3.66
0.20	9433	3.484	1349	5.5	3.55	3.36
0.20	9433	4.065	1117	5.5	3.55	3.45
0.25	8771	4.386	1069	8.8	3.39	3.11
0.25	8771	4.367	997	8.8	3.39	3.34
0.25	8771	4.149	974	8.8	3.39	3.60
0.30	7462	3.953	997	5.7	3.04	3.18
0.30	7620	4.255	884	5.7	3.04	3.30
0	14960	2.857	1857	0.77	4.83	4.69

IV TOTAL ENERGY DISTRIBUTION MEASUREMENTS FROM CLEAN SUBSTRATES

Work has continued on a literature review for suitable metals with which band structure effects may be examined by field emission techniques. Since the only band structure effects that can be detected by field emission are within 0.1 to 0.2 eV of the Fermi energy careful evaluation of theoretical band structure calculations must be made due to the uncertainties in determining positions of predicted band structure effects with respect to energy.

It was planned to examine at least one of the group Va metals such as Ta or Nb for a comparison with the neighboring group VIa elements W and Mo. A Ta rod was zone melted from which it was expected to be able to fabricate a field emitter; however, close examination showed the rod to be polycrystalline rather than single crystal. It is known to be possible to zone melt Ta and we are continuing the effort with the expectation that it will be possible to reorient the rod for use as field emission cathodes.

REFERENCES

1. C. Duke and M. Alferieff, J. Chem. Phys. 46, 923 (1967).

2. R. Gomer, J. Chem. Phys. 21, 1869 (1953).

3. R. Gomer, Field Emission and Field Ionization (Harvard University Press, Cambridge, Mass., 1961), p. 50.

4. A. van Oostrom, Philips Res. Suppl. (Netherlands) 11, 102 (1966).

5. L. Swanson and L. Crouser, Phys. Rev. Letters 19, 1179 (1967).

6. L. Swanson and L. Crouser, Phys. Rev. 163, 622 (1967).

7. R. Stratton, Phys. Rev. 135A, 794 (1964).

8. F. Itskovich, Soviet Phys. JEPT 23, 945 (1966).

9. D. Menzel and R. Gomer, J. Phys. Chem. 41, 3311 (1964).

10. L. Schmidt and R. Gomer, J. Chem. Phys. 42, 3573 (1965).

11. A. Bell and L. Swanson, Surface Sci. 10, 255 (1968).

12. J. Topping, Proc. Royal Soc. (London) A114, 67 (1927).

13. R. Young, Phys. Rev. 113, 110 (1959).

14. R. Good and E. Müller, Handbuch der Physik, (S. Flügge, Springer-Verlag, Berlin 1956) Vol. 21, p. 188.

15. R. Young and H. Clark J. Apply. Phys. Letters 9, 265 (1966).

16. F. Charbonnier and E. Martin, J. Appl. Phys. 33, 1897 (1962).

17. L. Schmidt, J. Chem. Phys. 46, 3830 (1967).

18. L. Swanson and R. Strayer, J. Chem. Phys. 48, 2421 (1968).